The 2009 IEEE/RSJ International Conference on
Intelligent Robots and Systems
October 11-15, 2009 St. Louis, USA

Development of Micro/Nano Displacement Sensor for Piezoelectric Actuator

Yong Yu, IEEE Member; Bo Song, IEEE Student Member; and Yunjian Ge

Abstract – **Micro displacement measurement of the PZT actuator is a micro sensor which could measure the minute displacement in micron or nanometer level. In general, the sensor is required to accommodate little space in order to save the room of measuring device. In this paper, a mechanical micro displacement sensor with smaller volume has been proposed. This paper focus on the whole process of this novel sensor from the working principle, parameter determine to the FEM simulation as well as the characteristic experiment and so on. This sensor can enlarge the displacement of the PZT by utilizing the lever principle and the strain gauges can perceive the variation without amplifying the noise. In this sensor, we use the flexure hinges as the rotation joints to obtain the expansion. Whatever the simulation results in FEM or the experiment data, both of which show that the sensor can perceive the displacement of the PZT actuator in micro/nano scale. Also, the characteristic experiment shows that the proposed sensor has a higher level linearity, resolution and lower error.**

Index Terms – Micro/nano displacement sensor*; *Flexure hinges*; *Strain gauges*; *Displacement expansion

I. INTRODUCTION

Piezoelectric actuator (PZT hereafter) has some advantages such as higher stiffness, faster response and smaller volume, all of which make it widely used in many micro/nano driving and location system, for instance, micro worktable, AFM (Atomic Force Microscope) [1], fluid control value and acoustical transducer. However, it still has several obvious disadvantages of which the most are hysteresis and nonlinear [2], so that the displacement measurement of PZT is required for PZT position control.

Various displacement measurements have been already used for acquiring the information of micro displacement [3][4][5]. Some of the measurement, for instance, laser interferometer with the optical principle need large space to fix, and couples of conventional measurements are not useful without an electric amplifier.

On the other hand, flexure hinges have already been used in precision machine design in manipulator and position plat-form as the passive transmission mechanism [6] [7] to obtain a relative large force, displacement or alter the direction of force unsophisticated. But, few of them have the ability to provide a larger expansion ratio between input and output displacements, where input displacement can be enlargedly transferred in nano-scale to output part and measured by the stain gauges, so that the initial input displacement could be acquired.

Meanwhile, strain gauge can acquire the deformation of an object for measuring a force or displacement directly, but it is not suitable to a micro environment since there is no enough deformation [8] [9]. Generally, an amplifier is needed to the micro environment, and there are two approaches. One is mechanical amplify device that uses the mechanical elements to enlarge the force or displacement; the other one is electronic magnification device which can magnify the output signal from the gauge. However, the deadly disadvantage of the electronic magnification is that it brings simultaneously the noise amplification while magnifying the input signal. It is nearly hard to tell the difference from the noise and the signal. Mechanical expansion also has its negative aspect that demands a higher stiffness to a measured object (see Fig.1). Fortunately, the stiffness of a PZT is high enough, so that it can make the mechanical expand to yield an enough deformation for being measured by strain gauge.

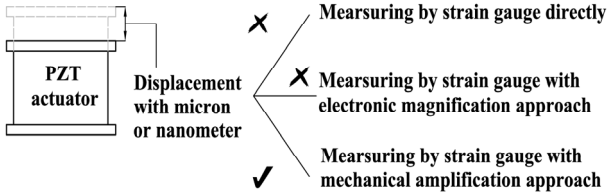

Fig.1 Considerable methods used strain gauges to measure the displacement of PZT

In this research, we consider utilizing the PZT's high stiffness to develop a displacement sensor for PZT. This sensor uses multi-stage enlarger configuration in order to acquire a larger expansion ratio, and transfer the expanded displacement into the elastic body in which the strain gauges could measure the change of deformation. With the output of strain gauges we could acquire the displacement information input by PZT. The PZT displacement sensor will be used for PZT position control, in order to solve the hysteresis and nonlinear which influence the performance of micro/nano PZT actuator system.

The mechanical configuration of the displacement sensor in this research is consist of some levers and hinges, where the levers could offer high stiffness as well as the function of displacement expansion that is also the essential point to this sensor. Traditionally, lever mechanism is an excellent mech-anism that could increase the displacement with enough stiffness. However, conventional hinges, which are used for connecting the levers to provide the rotation DOF, could not suitable for nano-scale displacement sensing. The first reason is that the friction of each hinges would occur unstably, which would influence the expansion ratio as well as input the larger noise especially for micro environment. Secondly, whichever

Yong Yu is with Department of Mechanical Engineering, Kagoshima University, Kagoshima 890-0065, Japan, yu@mech.kagoshima-u.ac.jp

Bo Song is with Institute of Intelligent Machine, Chinese Academy of Sciences, Hefei, Anhui Province, China and Department of Automation University of Science and Technology of China, Hefei, Anhui Province, China, song2006@mail.ustc.edu.cn

Yunjian Ge is with Institute of Intelligent Machine, Chinese Academy of Sciences, Hefei, Anhui Province, China, yjge@iim.ac.cn

the machining precision or the assembly accuracy is hard to ensure, so there are micro positional errors in hinges which will influence the lever's displacements especially in the micro environment. Finally the process of fabricating these minute hinges is rather complex and would waste countless time to fix them together.

This research considers using flexure hinges to solve these above problems. Using flexure hinge mechanisms can meet the requirements of high precision [10]. Flexure hinges gain their mobility from an elastic and plastic deformation exclusively. To achieve a high life cycle the deformation should be remained in the elastic strain. Fig. 2 shows a conventional flexure hinge, a cantilever beam with a circular notch, where the deformations will take place nearly only at the point of the smallest cross-section [11].

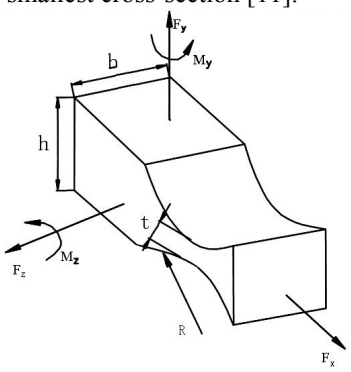

Fig.2 Uniaxial flexure hinge

This developed sensor can be used in AFM system, in which the displacement measurement based on the PZT deformation can be added in order to offer a feedback close-loop control system.

In the initial prototype, micro/nano displacement sensor offered a range of 5[μm] with the resolution of 3[nm] and the precision of nano-scale which can be usable in the feedback control of the AFM worktable. The effectiveness of the sensor is that a direct result of micro-measurement could also be realized by simple and traditional resistance strain gauges that means lots of expenditure can be saved as well as the space. In operation, the sensor works freely and peacefully without any friction due to the use of flexible hinges.

II. Configuration and Principle of Micro/Nano Displacement Sensor

A. Working principle

The destination of the mechanical expansion is to enlarge the displacement of PZT with the principle of lever mechanism. The ratio of magnification is essential to the whole configuration. Though the expansion ratio would be the larger the better, considering the size of the sensor body, we can not pick up a huge ratio for the reason that we should fix the PZT actuator inside the sensor tightly, as well as make sure the whole size is under control to be a smaller one which could be fixed in micro worktable. So, we choose multi-steps expansion just like Fig.3 shows, where several levers and hinges are utilized to construct a lever-hinge displacement expansion mechanism. Fig.3(A) illustrates a simplified section structure of the sensor. Fig.3(B) is a simplified model of Fig.3(A) and in this figure, we use lever AC instead of lever AB' and B'C. In Fig.3(C), we could find the deformations of every lever and hinge when there is an input displacement (δ_{in}).

The input displacement is imported at the hinge of B, and rotates lever AB' and B'C where two parts could be regarded as a one-lever rigid AC (Fig.3(B)) around hinge A, and the output displacement of hinge C is enlarged through the lever AC. This is the first enlarger stage. Simultaneously, relatives to lever DE we used CE as a transition lever. Hinge C could also be seemed as the input point of displacement which makes lever CE to rotate around the hinge C. Finally hinge E provides the input displacement to lever DE as well as the expanded displacement provides the output displacement of the upper end in elastic body FG which is a ratter thin flake. That is the second expansion stage. With limited DOF (Degree of Freedom) of lower end of the elastic body G which could be bent and acquire the topmost surface strain in the each end of elastic body and with the help of strain gauge pasted in the surface, we finally gain the perception of elastic body's deformation which reflects the input displacement by computing the expansion ratio of the whole system.

B. Expansion ratio

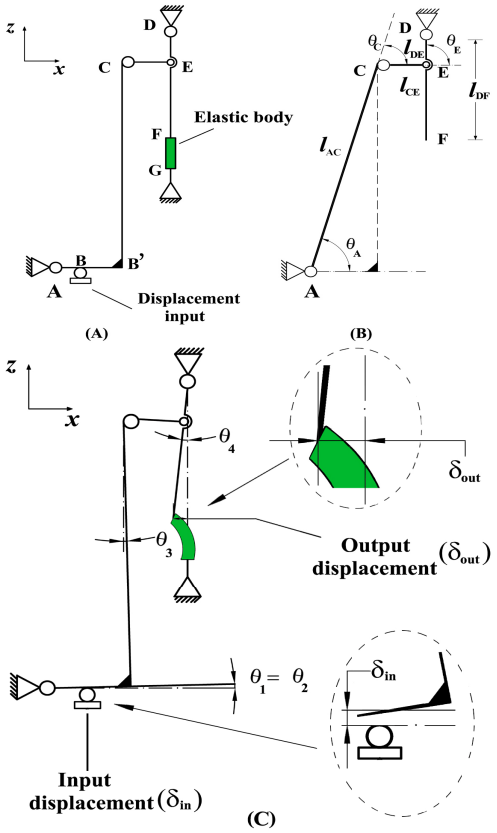

Fig.3 Lever-hinge displacement expansion mechanism

In order to compute total magnification ratio of the sensor, we set some parameters to the levers shown by Fig.3(A), l_{AB}= 1[mm], $l_{BB'}$=2[mm], $l_{B'C}$=15[mm], l_{CE} =2[mm], l_{DE}=1.5[mm], l_{AB}= 6[mm]. We simplify this figuration as a traditional four-bar linkage section (see Fig.3(B)) for obtaining kinematics

equation.

In Fig.3(B), we set $[x_A, y_A]^T$, $[x_C, y_C]^T$, $[x_E, y_E]^T$ and $[x_D, y_D]^T$ as the position vectors of joint A, C, E and D, l_{AC}, l_{CE}, l_{DE} as the length of each lever, and $\theta_A, \theta_B, \theta_C, \theta_D$, θ_E as the rotational angle of hinge A, B, C, D and E. We have

$$\begin{bmatrix} x_C \\ y_C \end{bmatrix} = \begin{bmatrix} x_A + l_{AC}\cos\theta_A \\ y_0 + l_{AC}\sin\theta_A \end{bmatrix}, \tag{2.1}$$

$$\begin{bmatrix} x_E \\ y_E \end{bmatrix} = \begin{bmatrix} x_C + l_{CE}\cos(\theta_C + \theta_A) \\ y_C + l_{CE}\sin(\theta_C + \theta_A) \end{bmatrix}, \tag{2.2}$$

$$\begin{bmatrix} x_D \\ y_D \end{bmatrix} = \begin{bmatrix} x_E + l_{ED}\cos(\theta_A + \theta_C + \theta_E \\ y_E + l_{ED}\sin(\theta_A + \theta_C + \theta_E) \end{bmatrix}. \tag{2.3}$$

Then we get the expression of x_D and y_D

$$\begin{bmatrix} x_D \\ y_D \end{bmatrix} = \begin{bmatrix} x_A + l_{AC}\cos\theta_A + l_{CE}\cos(\theta_C + \theta_A) + l_{ED}\cos(\theta_A + \theta_C + \theta_E) \\ y_A + l_{AC}\sin\theta_A + l_{CE}\sin(\theta_C + \theta_A) + l_{ED}\sin(\theta_A + \theta_C + \theta_E) \end{bmatrix}. \tag{2.4}$$

After the differential process, we get

$$\begin{bmatrix} -l_{AC}S_A - l_{CE}S_{AC} - l_{ED}S_{ACE} & l_{AC}C_A + l_{CE}C_{AC} + l_{ED}C_{ACE} \\ 0 & 0 \\ -l_{ED}S_{ACE} & l_{ED}C_{ACE} \\ 0 & 0 \\ -l_{CE}S_{AC} - l_{ED}S_{ACE} & l_{CE}C_{AC} + l_{ED}C_{ACE} \end{bmatrix}^T \begin{bmatrix} \Delta\theta_A \\ \Delta\theta_B \\ \Delta\theta_C \\ \Delta\theta_D \\ \Delta\theta_E \end{bmatrix} = \begin{bmatrix} \Delta x_D \\ \Delta y_D \end{bmatrix}, \tag{2.5}$$

where S_A, S_C, S_E, S_{AC}, S_{ACE} denote $\sin\theta_A$, $\sin\theta_C$, $\sin\theta_E$, $\sin(\theta_A+\theta_C)$, $\sin(\theta_A+\theta_C+\theta_E)$; C_A, C_C, C_E, C_{AC}, C_{ACE} denote $\cos\theta_A$, $\cos\theta_C$, $\cos\theta_E$, $\cos(\theta_A+\theta_C)$, $\cos(\theta_A+\theta_C+\theta_E)$ respectively for simple. $\Delta\theta_A$, $\Delta\theta_B$, $\Delta\theta_C$, $\Delta\theta_D$, $\Delta\theta_E$ are the angle displacement of θ_A, θ_B, θ_C, θ_D, θ_E. In Fig.3(C), we use θ_1, θ_2, θ_3, θ_4, denote $\Delta\theta_A$, $\Delta\theta_B$, $\Delta\theta_D$ and $\Delta\theta_E$.

Since $\Delta x_D = 0, \Delta y_D = 0$, and also we set the initial parameters as below,

$l_{AC} = 15.3[\text{mm}]$, $l_{CE} = 2[\text{mm}]$, $l_{ED} = 1.5[\text{mm}]$,

$\theta_A = 78.7[\text{deg}]$, $\theta_C = 0[\text{deg}]$, $\theta_E = 90[\text{deg}]$.

Accordingly, we obtain the expression from (2.5) as

$$\begin{bmatrix} -16.5 & 0 & -1.5 & 0 & -1.5 \\ 5 & 0 & 2 & 0 & 0 \end{bmatrix} \begin{bmatrix} \Delta\theta_A \\ \Delta\theta_B \\ \Delta\theta_C \\ \Delta\theta_D \\ \Delta\theta_E \end{bmatrix} = \begin{bmatrix} 0 \\ 0 \end{bmatrix}, \tag{2.6}$$

$$\begin{bmatrix} \Delta\theta_C \\ \Delta\theta_E \end{bmatrix} = -\frac{1}{2}\begin{bmatrix} 17 \\ 5 \end{bmatrix}\Delta\theta_A. \tag{2.7}$$

So, the output displacement in Fig.3 is

$$\delta_{out} = \Delta\theta_D l_{DF} = (\Delta\theta_A + \Delta\theta_C + \Delta\theta_E) l_{DF} = -75\Delta\theta_A. \tag{2.8}$$

$\Delta\theta_A$ is a rather micro displacement angle that could be closely equal to the value of $\tan\Delta\theta_A$, moreover

$$\Delta\theta_A \approx \tan\Delta\theta_A = \frac{\delta_{in}}{l_{AB}} = \frac{\delta_{in}}{1[\text{mm}]} = \delta_{in}. \tag{2.9}$$

So, we have $\delta_{in} = \Delta\theta_A$, and finally the total expansion ratio K_1 of the lever-hinge expansion mechanism can be expressed as

$$K_1 = \left|\frac{\delta_{out}}{\delta_{in}}\right| = \frac{75\Delta\theta_A}{\Delta\theta_A} = 75. \tag{2.10}$$

The above analysis is based on the assumption that all the levers are rigid bodies which means there is no deformation happened when they afford force or torque (We also build up other mathematic model which consider the materials deformation in another paper). Also, the flexure hinges we used here could be seemed as several torsion springs. These springs deposit energy when they have torsion deformation. So, this sensor could expand the input displace-ment and shows the measuring displacement, if the actuator, which output displacement support to be measured, could provide enough driving force as well as high rigid. PZT actuator belongs to this kind. Therefore, if we give a input displacement δ_{in}= 5[μm] along Z-axis direction, the terminal displacement output S_{max} of the sensor along X-axis direction is

$$S_{max} = K_1 \times \delta_{in} = 75\times 5[\mu\text{m}] = 375[\mu\text{m}]. \tag{2.11}$$

According to the lever magnification theory, when the PZT operator provides the input displacement $\delta_{in,}$ the angles of displacement of the hinges in Fig.3 are

$$\begin{cases} \Delta\theta_A = \Delta\theta_B = \dfrac{5\mu\text{m}}{1\text{mm}} = 5\text{mrad}, \\ \Delta\theta_C = -\dfrac{5}{2}\Delta\theta_A = -12.5\text{mrad}, \\ \Delta\theta_D = \Delta\theta_A + \Delta\theta_C + \Delta\theta_E = -50\text{mrad}, \\ \Delta\theta_E = -\dfrac{17}{2}\Delta\theta_A = -42.5\text{mrad}. \end{cases} \tag{2.12}$$

C. Input Force

Every flexure hinge could be simplified as a torsional spring. Consequently, we have

$$E = \frac{1}{2}K\Delta\theta^2, \tag{2.13}$$

$$T = K\Delta\theta, \tag{2.14}$$

where E and T are the energy and torque of torsional spring, and $\Delta\theta$ is the relative angle of rotations of the torsional spring. Based the law of conservation of energy, in the process of deformation recovery of the hinges, the work w_{in} by the elastic restoring force F_{in} is equal the deposited energy of all the flexure hinges and point E, where F_{in} is the force which can make point B on the sensor displace 5[μm] along Z-axis direction. If we use four of the lever-hinge expansion mechanisms which are arranged in parallel, the work w_{in} can be express as

$$w_{in} = F_{in}\cdot\delta_{in}, \tag{2.15}$$

$$w_{in} = E_{total} = 4\times\frac{1}{2}\left[K(\Delta\theta_A^2 + \Delta\theta_B^2 + \Delta\theta_C^2 + \Delta\theta_D^2 + \Delta\theta_E^2)\right], \tag{2.16}$$

$$F_{in} = 4\times\frac{K}{2}(\Delta\theta_A^2 + \Delta\theta_B^2 + \Delta\theta_C^2 + \Delta\theta_D^2 + \Delta\theta_E^2)\Big/\delta_{in} \tag{2.17}$$

$$= 8.975K[\text{N}],$$

where E_{total} is total energy that all the hinges preserved and K is the elastic coefficient of the flexure hinge to the hinge's rotation angle and will be discussed in next session, The force of PZT actuator could offer about 500[N] under nano lever displacing. We think that the PZT force can be far more beyond F_{in} so that this working principle we use to design the mechanism configuration is feasible under the quite large stiffness condition.

D. The hinges

Before the design of the hinges, it gives several hypotheses: (1) only the hinges suffer the elastic deformation and other parts of the frame are assumed as rigid body; (2) the flexure hinges cannot deform any more but the deformation of rotation.

Fig.2 shows the basic parameters of the uniaxial flexure hinge. The moment M_Z brings the deflection angle α_Z about Z axis of the uniaxial flexure hinge, and the simple form relationship [12] between them is

$$\frac{\alpha_z}{M_z} \approx \frac{9\pi}{2EbR^2(2\beta)^{5/2}} = \frac{9\pi R^{1/2}}{2Ebt^{5/2}}. \tag{2.18}$$

To the working hinges, the error of any β/γ can be under 1%, and the deformation takes place in the cross section of neck. Thus, the centre position of cutting-radius and the height of hinges are not key parameters except the centre cross section.

By the strain gauges attached in, we can get the displacement information. So we have

$$\frac{\alpha_z}{F_y} = R\sin\theta_m\left(\frac{\alpha_z}{M_z}\right) = R\sqrt{1-(1+\beta-\gamma)^2}\left(\frac{\alpha_z}{M_z}\right), \tag{2.19}$$

which can also be simplified as

$$\frac{\alpha_z}{F_y} \approx \sqrt{2\gamma-\gamma^2}\left(\frac{9\pi R^{3/2}}{2Ebt^{5/2}}\right). \tag{2.20}$$

A special hinge that we used is the centre of cutting radius on the edge of the hinge, so we have $h=2R+t$ and $\gamma=\beta+1$. Due to $\beta<<1$ and $\gamma\approx1$the former expression can be simplified as

$$\frac{\alpha_z}{F_y} \approx \frac{9\pi R^{3/2}}{2Ebt^{5/2}}. \tag{2.21}$$

Total deformation angel θ and deformation of hinges y are

$$\theta = \sum_{i=1}^{n}\Delta\theta_i, \tag{2.22}$$

$$y = \sum_{i=1}^{n}\Delta y_i, \tag{2.23}$$

where $\Delta\theta_i$ is the angle of rotation of ith hinge, Δy_i is the displacement of ith hinge, then we get

$$\frac{1}{\rho} = \frac{\frac{d^2y}{dx^2}}{\left[1+\left(\frac{dy}{dx}\right)^2\right]^{3/2}}, \tag{2.24}$$

where ρ is the curvature radius.

The travel of this sensor is rather small, and when the deformation happens, deflection is far more beyond the total length of the hinge. For the reason above, we get

$$\frac{dy}{dx} << 1, \tag{2.25}$$

$$\frac{1}{\rho} = \frac{d^2y}{dx^2}. \tag{2.26}$$

In the condition of the small angle of rotation, we can use $\theta\approx\tan\theta=dy/dx$, and converse the rectangular coordinate to polar coordinates, then the angle of rotation of flexure hinge can be expressed as

$$\theta = \int_0^{\pi}\frac{12MR\sin\alpha}{Eb(2R+t-2R\sin\alpha)^3}d\alpha. \tag{2.27}$$

We use MATLAB to solve this integral and get the angle of rotation stiffness of the hinge M/θ under different t and R (see Table 1).

R and t are the crucial parameters of the hinge. Giving a great value of t and a small value of R, the stiffness, dynamic performance and anti-interference properties are superior. On the contrary, the sensitivity and resolution are splendid when t is bigger and R is smaller. It is a dilemma. Our sensor is working for measuring the micro displacement and force not for transmission. Consequently, it is vital to ensure the sensitivity and resolution of the sensor, for which we choose to increase R and decrease t, simultaneously considering the response frequency which also restricts R, in addition the thickness of the hinge should be more than 0.3[mm] because of the wire cutting process, we choose 0.5[mm] as the value of parameter t, 3[mm] as the value of parameter b.

TABLE I ANGLE OF ROTATION STIFFNESS OF THE HINGE

	t=0.1mm	t=0.2mm	t=0.3mm	t=0.4mm	t=0.5mm
R=1.0mm	2.266e-4Eb	0.0013 Eb	0.0036 Eb	0.0075 Eb	0.0134 Eb
R=0.5mm	3.247e-4 Eb	0.0019 Eb	0.0053 Eb	0.0112 Eb	0.0201 Eb
R=0.4mm	3.654e-4 Eb	0.0021 Eb	0.0061 Eb	0.0129 Eb	0.0232 Eb
R=0.3mm	4.267e-4 Eb	0.0025 Eb	0.0073 Eb	0.0155 Eb	0.0281 Eb
R=0.2mm	5.343e-4 Eb	0.0032 Eb	0.0094 Eb	0.0204 Eb	0.0375 Eb

E. The Configuration of the Sensor

The displacement sensor is capable of measuring the micro displacement by means of measuring the input force. Thus it is very essential for the sensor to have a peculiar structure to expand the displacement. As is shown in Fig.4, the figuration of the sensing element for the displacement sensor is composed of a monolithic cube shell in which we cave the hinges, members as well as the elastic body through the wire cutting technology. Posing a PZT inside the sensor, simultaneously holding the upper surface of the PZT connected firmly with roof of sensor, we can acquire the displacement information by the roof which is a solo axis displacement. By a series of members and flexure hinges in the surface of the sensor the micro displacement can be enlarged and transferred to the elastic body. Here, we use the flexure hinges not only as the displacement amplified tool but as energy storage cells by using which the deformation could be resumed immediately when the displacement is given by

the PZT dismiss, and without which the sensor would not operate in real time. Consequently, the measure sensitivity and the real time response of the sensor are increased.

In order to make the force and moment balance, the micro/nano displacement sensor is designed symmetrically. It has a converse symbol T member connected to the roof, though which the force and the displacement can be transferred to the both side of each of the sensor's working surface, and then two couples of members and flexure hinges enlarge the displacement in each side. The elastic body is an extraordinary thick fleet which is only 0.3[mm] width and connect the two members in its each side. The elastic body is not a solo one that needs paste to the members but as one of the entity of the whole sensor that means after the process of wire cutting it appears automatically.

F. The Material of the Sensor

For the reason that the elastic body is thicker than the other parts so the strain is centralize in this part, the material must have excellent ability of elastic recovery and stiffness. The material of this sensor is desired considering cautiously, in respect that the thickness of our hinges and elastic body is rather minute, if the material cannot afford the enormous strain, some of them may be broken down. Though most of the force and displacement sensors using elastic body are made of aluminium alloy, alloy steel, spring steel and QBe2 that could provide sensitive and stiffness simultaneously in some certain, such common material can not deal with this very kind of displacement sensor because of the huge strain. We choose the 35CrMnSiA as the material of the sensor for its higher strength limit and elastic modulus ratio, especially for that it is rather suit for fabricate high precision element, and its density is 8.23[kg/m^3],and Poisson radius is 0.28.

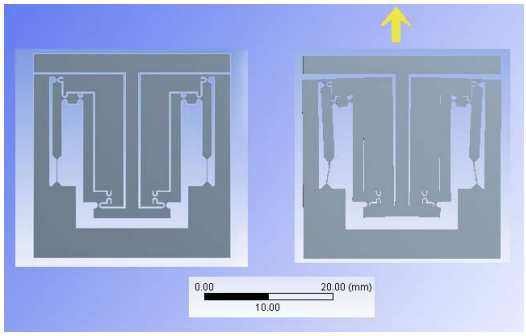

Fig.4 Flexure hinge works though the structure deformation

The maximal stress would be happen in the section which takes place the greatest angle of rotation $\theta_{\max}$, from which

$$\sigma_{\max}=\frac{M_{\max}}{W}=\frac{K\theta}{\frac{1}{6}bt^2}<[\sigma]=\frac{\sigma_s}{n_s}, \qquad (2.28)$$

where σ_s is the yield limit of the material, n_s is the safety factor (usually 1.5~2.2 for sensitive material). By (2.30) the maximal deformation angel of the hinges using sensitive material can be express as

$$\theta=\frac{\sigma_s}{n_s}\cdot t^2\cdot\frac{b}{6K}. \qquad (2.29)$$

The value of K we set is 0.0053Eb from Table 1 as well as b=3[mm], t=0.3[mm], R=0.5[mm], and safety factor n_s =1.5. Afterward, we get that the allowable angel of 35CrMnSiA is 12.4[mrad], which is great higher than other traditional material.

III. FEM Simulation

In order to select the appropriate position of each strain gauge and to give a scientific evaluation on measure sensitivity and resonance frequencies of this sensor, it is very essential to realize the structural behaviour of the sensing element. The sensing element of the sensor is monolithic with a rather complicated configuration, thus it is hard to provide a pure theory accurately about the solid mechanics but to use the FEM simulations which can perform to determine the strain distribution of the elastic body as well as get the resonance frequency of the sensor [13].

The main size of the sensing element model is 38[mm] ×38[mm]×38[mm], all the radius and the width of working flexure hinges are R_n=0.5[mm], and W_n=2[mm]; the thickness of all the element in the working surface is T_n=3[mm]; the width and length of the elastic body are W_{EF}=0.2 [mm] and L_{EF} =3.85[mm]; the thickest part of the flexure hinges is t= 0.3[mm].The finite element model is meshed with smart mesh division then refines the parts which we are interested in, for instance, the elastic body and flexure hinges. The material elastic modulus E=210×10^9 [Pa], Poisson's ratio μ = 0.28, and the density is 8.23 ×103 [kg/m^3].

The FEM simulations are implemented in the condition of that a displacement is applied to the roof of the sensor using which simulated the displacement of PZT which should be inside the sensor. The displacement applied in the analysis is S_Z =0.005[mm].

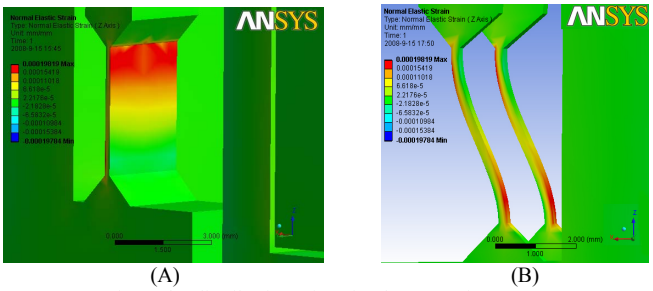

(A) (B)

Fig.5 The distribution of strain along Z-axis

Fig.5 shows the distribution of strain along Z-axis under the displacement along Z-axis S_Z=5[μm] of the elastic body in which we paste the strain gauges.

There are both negative and positive strain parts in the same elastic body, which means the deformation the body seems like the symbol S. From the positive part in the upper body to the positive part in the lower body the strain gradient has a perfect distribution. Furthermore in the back of the body the strain distribution is just opposite which means when the strain in one face of the body is positive, the other face of the elastic body do have the negative strain, and vice versa. The maximal positive strains (≈1.98×10^{-4}) and relative larger negative

strains (≈ -1.38×10^{-4}) of the sensor happen in the each endpoint of the elastic body.

TABLE II MODE AND RESONANCE FREQUENCY

Mode	Frequency (Hz)	Shape Description
1	122.62	Rotation about Z axis
2	377.26	Rotation about X axis
3	434.89	Rotation about Y axis
4	712.18	Deflection in Z direction
5	1304.90	Deflection in X direction
6	1354.00	Deflection in Y direction

In Table II, the mode analysis of this sensor has been introduced, and the mode numbers from one to six denote the order number of each process of mode analysis.

IV. CHARACTERISTIC EXPERIMENTS AND DISCUSSION

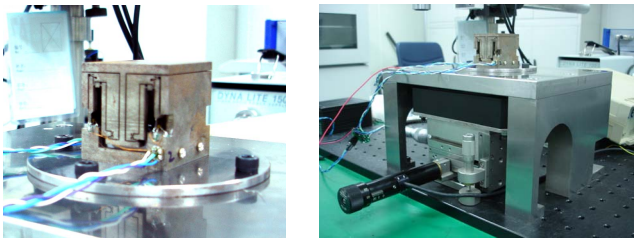

Fig.6 The prototype displacement sensor

The prototype micro/nano displacement sensor (see Fig.6) was manufactured according to the FEM model. A series of experiments have been done in order to validate the FEM simulations and to evaluate the performance of the sensor. Fig.7 shows the schematic diagram of the experimental setup. The displacement sensor was fixed on a calibration table which is consisted of a manual coarse adjustment table, an accurate nano-positioning table and date processing module. The resistance strain gauges which sensitivity coefficient is 2.0 we used here are pasted on the surfaces of elastic body where the maximum strain happened in our FEM simulation. In order to record the data rapidly and conveniently, xPC Target which is a new MATLAB toolbox is used to track the signal of dynamic performance. Also PCL818HG is used for a converter of A/D, INA122 as an amplifier and MCU 8051F040 with a CAN interface is used for data processing.

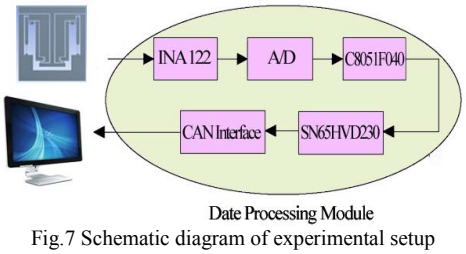

Fig.7 Schematic diagram of experimental setup

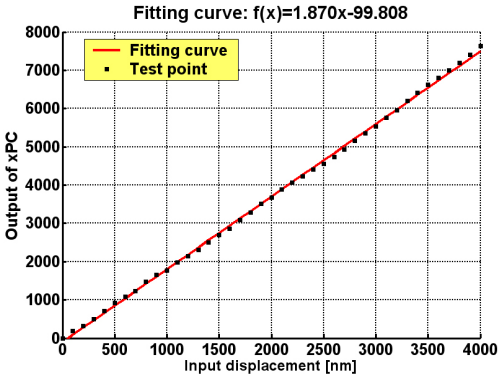

Fig.8 Experiment result and fitting curve for 100[nm] interval

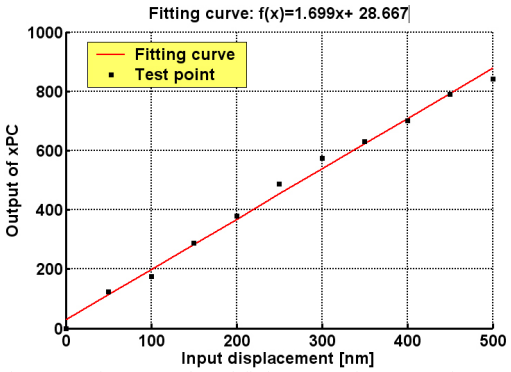

Fig.9 Experiment result and fitting curve for 50[nm] interval

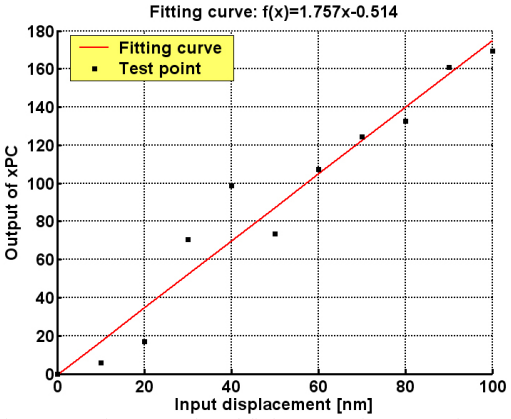

Fig.10 Experiment result and fitting curve for 10[nm] interval

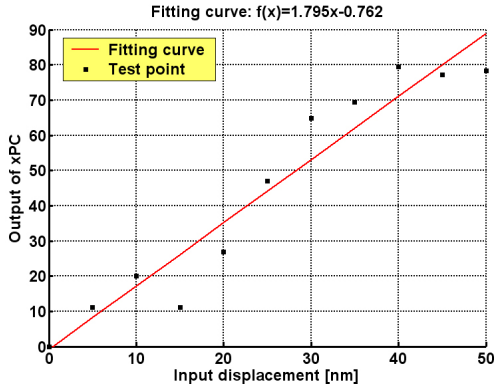

Fig.11 Experiment result and fitting curve for 5 [nm] interval

A. Static Performance

The whole process of calibration takes part in the overall measurement system based on the Nano-Positioning and Scanning System (P517) developed by PI Company in Germany and it is showed in Fig. 8. The P517 provides a scan scale of 0.03[mm], the closed-loop resolution is 0.1[nm] and full–range repeatability is 5%. We use the P517 to provide the nano-scale displacement and read the number from the xPC which also equals the voltage output of the sensor. Also, a fitting curve simultaneously is added in order to form a set of control, from which we can know that whether the linearity of the sensor is superior or not.

At the beginning of the static performance experiment (see Fig.9, for example), we set the sensor into an initial condition which already has a contact between the sensor and the P517, and then we load the displacement 50[nm] by 50[nm], finally up to the 500[nm] which is a rather safe displacement to this sensor. Contemporarily, the xPC displace the output number of sensor on the computer screen.

The nonlinear error is 1.6%, 4.1%, 12.7% and 15.0% from the interval scale of 100[nm], 50[nm], 10[nm] and 5[nm] with the total range of each process is 0~4000[nm], 0~500[nm], 0~100[nm] and 0~50[nm] (see Fig.9, 10, 11 and 12). The resolution of the whole sensor could be reach as high as 5[nm].

B. Sensor Performance Analysis

The calibration experiment is in the foundation of displacement input and the voltage output, and from which we could see that the nonlinearity usually happens in the initial steps of the measurement scale. Consequently, we could use the relative superior segment to measure the displacement. Taking the experiment with 50[nm] interval (see Fig.9) as an example, after remove the last three points the nonlinear error could be decreased as low as 3.4%. Also this nonlinear phenomenon probably due to that the machining accuracy of the sensor and the location of strain gauge are not easy to achieve the design parameters accurately. Besides, another reason for the nonlinear error happening is the noise interference. Also how to promote the ability of noise reduction deserver to be further considered. In addition, some details such as the configuration of the elastic body and the position of the gauges are still need to change in order to obtain superior performance.

V. CONCLUSIONS

A novel micro/nano displacement sensor using levers and flexure hinges and based on strain gauges is presented in this paper. The sensor can measure the micro displacement linearly with low error. The stiffness, distribution of the strains and the expansion ratio are computed either by the theory or the FEM simulations. The static displacement experiments were carried out from which the performance of the sensor is almost uniform to simulation result. This nano/micro displacement sensor provides superior sensitivity and nano-level resolution with simple structure and a minute nonlinearity in the working range. In the future work, we design to set a series of more powerful processing circuits, and a structure optimization is also needed, by which we can promote the precision and linearity of the whole sensor.

REFERENCES

[1] G. Binnig, C. F. Quate and C. Gerber, "Atomic force microscope," *Physical Review Letters*, vol. 56, pp. 930-933, 1986.

[2] S. B. Jung and S. W. Kim, "Improvement of scanning accuracy of PZT piezoelectric actuators By Feedforward Model-Reference Control," *Precision Engineering-Journal of the American Society for Precision Engineering*, vol. 16, pp. 49-55, 1994.

[3] Y. Liu and T. Higuchi., "Precision Positioning Device Utilizing Impact Force of Combined Piezo-Pneumatic Actuator," *IEEE/ASME Transactions on Mechatronics*, vol. 6, pp. 467-473, 2001.

[4] E. K. Chan and R. W. Dutton, "Electrostatic micromechnical actuator with extended range of travel," *J. Microelectromech. Syst.* Vol. 9, pp. 321-328, Sept. 2000.

[5] Y. Yu, T. Ishitsuka and S. Tsujio, "Torque Sensing of Finger Joint Using Strain-Deformation Expansion Mechanism," *Proceedings of IEEE International Conference on Robot and Automation*. vol. 2, pp. 1850-1856, 2003.

[6] B. J. Yi and G. B. Chung, "Design and experiment of a 3-DOF parallel micromechanism utilizing flexure hinges," *Robotics and Automation, IEEE Transactions on Publication*. vol.19, No. 4, pp. 604-612, 2003.

[7] J. Schlick and D. Zuehlke, "Smart Tong Grippers for Micro-Parts," *Smart Sensors, Actuators, and MEMS, Proceedings of the SPIE.* Vol. 5116, pp. 220-228. 2003.

[8] K. Mizutani, T. Kawano, and Y. Tanaka, "A piezoelectric-drive table and its application to micro-grinding of ceramic materials," *Precision Engineering-Journal of the American Society for Precision Engineering*, vol. 12, pp. 219-226, 1990

[9] Y. Yu, T. Chaen and S. Tsujio, "High-Stiffness and High-Sensitivity 3-Axis Force Sensor Using Strain-deformation Expansion Mechanism," *Proceedings of IEEE International Conference on Intelligent Robots and Systems*. pp. 4417-4422, 2006.

[10] J. P. Bacher, S. Bottinelli, J. M. Breguet and R. Clavel, "Delta(3): design and control of a flexure hinges mechanism," *Microrobotics and Microassembly Iii.* vol. 4568, pp. 135-142., 2001.

[11] J. Hesselbach and A. Raatz, "Pseudo-elastic flexure-hinges in robots for micro assembly," *Microrobotics and Microassembly Ii*. vol. 4194, pp. 157-167, 2000.

[12] S.-F. Xue, Q.-X. Li. *Design of Precision instruments*, Beijing Tsinghua publishing house, pp. 203-210, 1991. (*in Chinese)*

[13] M. Meng, Z.-C. Wu Y. Yu, Y. Ge, and Y.-J. Ge, "Design and characterization of a six-axis accelerometer," *Proceedings of IEEE International Conference of Robotics and Automation,* pp. 2356-2361, 2005.